HVAC analysis of a building installed shape-stabilized phase change material plates coupling an active building envelope system

Bor-Jang Tsai [1]、Sheam-Chyun Lin[2] and Wei-Cheng Yang[3]

[1, 3] Department of Mechanical Engineering
Chung Hua University
No. 707, Sec. 2, WuFu Rd., HsinChu, Taiwan.
e-mail: bjtsai@chu.edu.tw

[2]Department of Mechanical Engineering
National Taiwan University of Science and Technology
No. 43, Sec.4, Keelung Rd.,Taipei, Taiwan.
e-mail: sclynn@mail.ntust.edu.tw

Abstract : Shape-stabilized phase change material (SSPCM) plates combined with night ventilation in summer is investigated numerically. A building in Hsinchu, Taiwan without active air-conditioning is considered for analysis, which includes SSPCM plates as inner linings of walls、the ceiling and floor, and an active building envelope system (ABE) is installed as well in the room becomes the Hybrid system. In the present study, a kind of floor with SSPCM is put forward which can absorb the solar radiation energy in the daytime or in summer and release the heat at night or in winter. In this paper, the thermal performance of a room using such floor、wall and ceiling were numerically studied. Results show that the average indoor air temperature of a room with the SSPCM floor was about 2 K to 4 K higher than that of the room without SSPCM floor, and the indoor air temperature swing range was narrowed greatly. This manifests that applying SSPCM in room suitably can increase the thermal comfort degree and save space heating energy in winter.

Key-Words : Shape-stabilized phase change material, Active building envelope system, HVAC, Renewable energy

1 Introduction

Energy storage not only reduces the mismatch between supply and demand but also improves the performance and reliability of energy systems and plays an important role in conserving the energy [1, 2]. It leads to saving of premium fuels and makes the system more cost effective by reducing the wastage of energy and capital cost. One of prospective techniques of storing thermal energy is the application of phase change materials (PCMs). Unfortunately, prior to the large-scale practical application of this technology, it is necessary to resolve numerous problems at the research and development stage. One of problems is so called the Stefan problem [3]. The heat transfer characteristics of melting and solidification process arise in the presence of phase change and expressing the energy conservation across the interface. In literature, this solid-liquid interface boundary is known as Stefan or moving boundary problem. It may have low conduction heat transfer.

1.1 Shape-Stabilized PCM (SSPCM)

In recent years, the Stefan problem has been resolved, a kind of novel compound PCM, the, Shape-stabilized PCM (SSPCM) has been attracting the interests of the researchers [4–6]. Fig. 1 shows the picture of this PCM plate. It consists of paraffin as dispersed PCM and high-density polyethylene (HDPE) or other materials as supporting material. Since the mass percentage of paraffin can be as much as 80% or so, the total stored energy is comparable with that of traditional PCMs.

Zhang et al. [7] investigated the influence of additives on thermal conductivity of SSPCM and analyzed the thermal performance of SSPCM floor for passive solar heating. To the authors' knowledge, no research work reported in the

literature has made on the performance of shape-stabilized PCM application coupling the active building envelope system (ABE) in buildings combined with night ventilation. Therefore, the purpose of this study is to perform a numerical analysis on the thermal effect of shape-stabilized PCM plates as inner linings on the indoor air temperature under night ventilation conditions in summer, coupling the ABE system in a building, and for overall system of the building based upon a simulated room; a generic enclosure, combined with the climate report of Hsinchu city, Taiwan, 0am~24pm, 1st ~6th July., 2008. [8] to investigate: (1) feasibility study of the hybrid system (2) heating capability analysis (3) cooling capability analysis (4) indoor temperature levels. For the sake of simplification, thermal performance is the only consideration.

Several applications and system design of building can be seen in papers of the NAUN/WSEAS journals and proceedings [9-11]

1.2 Active Building Envelopes

A brief description of the proposed ABE system is provided here (see Fig. 2). For more details, see [12]. The ABE system is comprised of two basic components: a photovoltaic unit (PV unit) and a thermoelectric heat pump unit (TE unit). The PV unit consists of photovoltaic cells, which are solid-state devices that convert solar radiation energy into electrical energy. The TE unit consists of thermoelectric heaters/coolers (referred to here onwards as TE coolers), which are solid-state devices that convert electrical energy into thermal energy, or the reverse. The PV and the TE units are integrated within the overall ABE enclosure. As shown in Fig. 2, the PV unit forms an envelope surrounding the external wall such that a gap is maintained between the wall and the PV unit. This gap acts as an external heat dissipation zone for the TE unit. The external walls of the proposed ABE system consist of two layers, as shown in Fig. 2. The external layer (facing the PV unit) is made of a thermal insulating material, and the internal layer is made of a material with high heat storage capacity. In Fig. 2, the words ‘‘Thermal insulation’’ and ‘‘Thermal Mass’’ pertain to the external and the internal layers of the ABE wall, respectively. The TE coolers/heaters are dispersed inside the openings that are provided in the insulating layer. Each TE cooler/heater consists of two heat sinks. As shown in Fig. 2, the internal heat sink either absorbs or dissipates heat to the thermal mass layer. The external heat sink either absorbs heat from, or dissipates heat to, the surrounding air; through natural or forced convection.

The author’s team; Tsai BJ [13] just finished a project; In a building installed the ABE system without SSPCM, wind、solar driven, bypass the windmill flow as a air flow (as shown Fig. 3), ambient temperature, To is equal to 308 K and indoor temperature, Ti is 301 K. Numerical results show the Ti will decrease 2 K when the ABE operating with heat sinks, without fan. As fan is opened, strong convective heat transfer, Ti will decrease approximately 4~5 K.

1.3 Hybrid system

Zhou et al. [14] in 2009 reported effect of shape-stabilized phase change material (SSPCM) plates in a building (as shown Fig. 4) combined with night ventilation in summer is investigated numerically. Their conclusions show that the SSPCM plates could decrease the daily maximum temperature by up to 2 K due to the cool storage at night. Under the present conditions, the appropriate values for melting temperature, heat of fusion, thermal conductivity and thickness of SSPCM plates are 26 C, 160 kJ kg^{-1}, 0.5Wm^{-1} C^{-1} and 20 mm, respectively. The ACH at night needs to be as high as possible but the ACH at daytime should be controlled.

1.4 Literature Survey Of Numerical Techniques

During the phase change the solid–liquid interface moves away from the heat transfer surface. The difficulty in solving a phase change problem is the presence of a moving boundary or region on which heat and mass balance conditions have to be met. Generally, two approaches of the finite difference and finite element techniques are used to solve the phase change problems numerically. One of the methods to solve the moving boundary problem is enthalpy formulation [15, 16]. The enthalpy method is used in a particular way so that the only unknown variable is the temperature of the phase change material and the solidification occurs at a uniform temperature. In this work we use the modified enthalpy method treats the enthalpy as a

temperature dependent variable and constructs the latent heat flow through the volume integration with the use of the enthalpy of the system [17, 18]. Heat transfer with moving boundary involving phase change is very important in latent heat storage application, i.e., ice formation, freezing of food, castings, metallurgy, crystal growth and various other solidification techniques. The predication of temperature distribution and rate of melting or solidification is very important in order to design such storage device.

2 Analysis Method—Physical And Mathematic Analysis And Modeling

The analysis is designed to examine the indoor thermal comfort level under night ventilation when the SSPCM plates are used or not. A typical south-facing middle room (room A shown in Fig. 5) in a multi-layer building in Hsinchu city, Taiwan, is considered as the model room for analysis, which has only one exterior wall (the south wall) and others are all interior envelopes. The dimension of the room is assumed as 3.9 m (length) x 3.3 m (width) x 2.7 m (height). The south wall is externally insulated with 60-mm-thick expanded polystyrene (EPS) board. There are a 2.1 m x 1.5 m double-glazed window and 1.5 m x 1.5 m ABE system in the south wall and a 0.9 m x 2 m wood door in the north wall which is adjacent to another room or the corridor. The overall heat transfer coefficients of the window and door are 3.01 and 0.875Wm^{-2} C^{-1}, respectively. SSPCM plates are attached to inner surfaces of four walls and the ceiling as linings. Based on a practical consideration, no SSPCM is included in the floor structure. Thermo-physical properties of SSPCM and materials of building envelopes are shown in Table 1. The phase transition temperature range of SSPCM is assumed to be 1 K. Natural ventilation in the day and mechanical ventilation at night are considered. The total indoor heat produced by the equipments, furniture, light and occupants, etc. is assumed to be 50W (average value over the day). The summer climate data is generated by the software Medpha [8]. A verified enthalpy model [19] is applied for this simulation.

2.1 Heat Transfer Model Of SSPCM Wall And Ceiling

The schematic of heat transfer through the exterior wall is shown in Fig. 6. The transient enthalpy equation is

$$\rho_j \frac{\partial H}{\partial t} = k_j \frac{\partial^2 T}{\partial x^2} \quad (1)$$

where for SSPCM, $H = \int_{T_0}^{T_1} c_{p,s} dT + \int_{T_1}^{T_2} c_{p,m} dT + \int_{T_2}^{T} c_{p,l} dT$,

for the insulation layer and the hollow brick layer,

$$\begin{cases} \rho_j = \rho_i, \quad k_j = k_j, \quad c_{p,j} = c_{p,i} & 0 \le x < x_1 \\ \rho_j = \rho_b, \quad k_j = k_b, \quad c_{p,j} = c_{p,b} & x_1 \le x < x_2 \\ \rho_j = \rho_p, \quad k_j = k_p & x_2 \le x < x_3 \end{cases}$$

The initial condition is

$$T(x,t)_{t=0} = T_{init} \quad (2)$$

For the surfaces exposed to the outside and inside air, the boundary conditions are

$$q_{r,out} + h_{out}\left(T_{out} - T_{i,out}\right) = -k_i \left.\frac{\partial T}{\partial x}\right|_{x=0} \quad (3)$$

$$q_{r,in} + h_{in}\left(T_{in} - T_{i,in}\right) = -k_p \left.\frac{\partial T}{\partial x}\right|_{x=x_3} \quad (4)$$

For the exterior wall, $q_{r,in}$ and $q_{r,out}$ are indoor and outdoor radiation heat flux, respectively (Fig. 6). The convective coefficients h_{out} and h_{in} are calculated according to the ASHRAE Handbook [20].

The above equations are also applicable to interior walls and the ceiling. For the interior walls, h_{out} and $q_{r,out}$ are zero. For the ceiling (Fig. 7), the surface at $x = 0$ is assumed insulated and the inner surface corresponds to convective heat transfer coefficient h_c and thermal radiation $q_{r,c}$. Thermal radiations among the internal surfaces of walls, floor and ceiling are calculated by thermal radiation network method [21].

2.2 Heat Transfer Model Of The SSPCM Floor

For floor construction shown in Fig. 8, the transient heat transfer equation is

$$\rho_j c_{p,j} \frac{\partial T}{\partial t} = k_j \frac{\partial^2 T}{\partial y^2} \quad (5)$$

ρ_j, k_j and $c_{p,j}$ are as follows:

$$\begin{cases} \rho_j = \rho_i, \quad k_j = k_j, \quad c_{p,j} = c_{p,i} & 0 \le y < y_1 \\ \rho_j = \rho_a, \quad k_j = k_a, \quad c_{p,j} = c_{p,a} & y_1 \le y < y_2 \\ \rho_j = \rho_f, \quad k_j = k_f \quad c_{p,j} = c_{p,f} & y_2 \le y < y_3 \end{cases}$$

Again, the initial condition is

$$T(y,t)_{t=0} = T_{init} \quad (6)$$

The boundary conditions are

$$\begin{cases} k_i \left.\frac{\partial T}{\partial y}\right|_{y=0} & y=0 \\ -q_{gap} + \varepsilon\sigma\left(T_{i,un}^4 - T_{i,up}^4\right) = k_i \left.\frac{\partial T}{\partial y}\right|_{y=y_1} & y=y_1 \\ -q_{gap} + \varepsilon\sigma\left(T_{i,up}^4 - T_{i,un}\right) = k_f \left.\frac{\partial T}{\partial y}\right|_{y=y_2} & y=y_2 \\ q_{f,up} + h_f\left(T_{in} - T_{f,up}\right) = k_f \left.\frac{\partial T}{\partial y}\right|_{y=y_3} & y=y_3 \end{cases} \quad (7)$$

Where $q_{f,up}$ is the radiation heat flux from the walls and ceiling to the wood floor; for the air gap, heat flux q_{gap} be calculated by the following equation [22]:

$$q_{gap} = N_u \frac{k_a}{L_{gap}}\left(T_{i,up} - T_{f,un}\right) \quad (8)$$

Where $T_{i,up}, T_{f,un}$ are the temperature at the upper surface of the insulation layer and at the under surface of the wood floor respectively. And N_u (Nusselt number) is calculated by the following equation:

$$N_u = \begin{cases} 0.212\left(Gr_L P_r\right)^{1/4}, & Gr_L = 1\times10^4 - 4.6\times10^5 \\ 0.061\left(Gr_L P_r\right)^{1/3}, & Gr_L > 4.6\times10^5 \end{cases} \quad (9)$$

When Gr_L is less than 10^4, only thermal conductivity is considered.

C. Model of the indoor air of hybrid system building

The energy conservation equation fir the indoor air is

$$c_{p,a}\rho_a V_R \frac{dT_a}{dt} = \sum_{i=1}^{N} Q_{w,i} + Q_{s,c} + Q_L + Q_{win} + Q_{ABE} \quad (10)$$

Where $Q_{S,C}$ is assumed 70% of the total energy from the heat source [23], and $Q_{w,i}, Q_L$ and Q_{win} QABE [12,13] are calculated by the following equations:

$$Q_{win} = h_{in} \times \left(T_{w,i} - T_{in}\right) \times A_{w,i} \quad (11)$$

$$Q_L = c_{p,a}\rho_a V_R \times ACH \times \left(T_{out} - T_{in}\right)/3600 \quad (12)$$

$$Q_{win} = U_{win} \times \left(T_{out} - T_{in}\right) \times A_{w,i} \quad (13)$$

$$Q_{ABE} = Q_{ph} = Q_{pc} + IV \quad (14)$$

D. Model of the SSPCM

The phase change model is based on the enthalpy method as modified by Zivkovic and Fujii [24]. They split the enthalpy as sensible and latent heats and included the melting fraction f in the one-dimensional transient heat equation as given in Eq. (18) below,

$$H = h + L.f_1 \quad (15)$$

Where, $h = \int_{T_m}^{T} cdT$

The local liquid fraction f_1: is given as,

$$f_1 = \begin{cases} 0 \;\; if \;\; T < T_m, (Solid) \\ 1 \;\; if \;\; T > T_m, (Liquid) \\ druing \;\; melting \;\; or \;\; solidification \;\; of \;\; the \;\; CV \\ f_1 \;\; is \;\; time \;\; dependent \;\; and \;\; between \;\; 0 \;\; and \;\; 1 \end{cases}$$

Substituting in the one dimensional transient heat equation for constant conductivity, density, specific heat gives

$$c\frac{\partial T}{\partial t} = \frac{k}{\rho}\frac{\partial^2 T}{\partial x^2} - L\frac{\partial f_1}{\partial t} \quad (16)$$

The whole domain of the rectangular storage is partitioned in N equidistant nodes. The control volume (CV) associated with each node has a thickness Δx, while nodes 1 and N have half-thickness ($\Delta x/2$).

3 Numerical Technique

3.1 Description Of The Model Room

The model room for analysis, which has dimension assumed as 3.9 m (length) x 3.3 m (width) x 2.7 m (height) concrete chamber. The thickness of chamber is 300mm, except the floor and the south wall each wall was installed 50mm thick SSPCM. The south wall is externally insulated with 60-mm-thick expanded polystyrene (EPS) board. There are a 2.1 m x 1.5 m double-glazed window and 1.5 m x 1.5 m ABE system in the south wall and a 0.9 m x 2 m wood door in the north wall which is adjacent to another room or the corridor. Floor is made of the first 30mm thick wood layer, under that the second layer is 40mm SSPCM layer, in between is the air layer with 30mm thick. And the extended computational domain is six times larger than that of the model room. (see Fig. 9, Fig. 10)

3.2 Input Parameters Of The Model Room And Applying Software

In this study, using the Gambit to construct the solid model and grid mesh, then applying the Fluent as the solver of flow and thermal field. All parameters of the building and material properties of SSPCM were tabulated in Table 1. Regarding conditions of outside environments of the model room were listed in Table 2.

3.3 Establish Grid Cells

Cells of grid mesh of this model room as Fig. 11.

Outside environment (7505.784 m^3)：188520 cells

Concrete layer (11.565 m^3)： 285517 cells

SSPCM layer (2.364 m^3)：154989 cells

Inside air of room (18.72 m^3)：149760 cells

Floor-wood layer (0.2673 m^3)：7128 cells

Floor-air gap layer (0.2673 m^3)：7128 cells

Floor-SSPCM layer (0.3564 m^3)：7128 cells

Door-wood (0.09 m^3)：720 cells

Window-glass (0.21 m^3)：1680cells

Air layer front glass window (1.26 m^3)：4320 cells

Air layer front wood door (0.54 m^3)：10,080 cells

3.4 Settings Of The Fluent

Settings of the Fluent software as below:

1. Solver：Segregated
2. Space：3D
3. Velocity Formulation：Absolute
4. Gradient Option：Cell-Based
5. Formulation：Implicit
6. Time：Unsteady
7. Unsteady Formulation：1st-Order Implicit
8. Porous Formulation：Superficial Velocity

3.5 Initial Conditions

The energy stored in cycle is: absorption heat

The ambient temperature is 303 K, 1atm and temperature of SSPCM layer is assuming a constant temperature 293 K, the optimal time (ie. Melting/fusing temperature, and its latent capacity is 265MJ/m^3。The initial condition (t=0) of indoor air temperature is assuming 303 K。 On the contrary,

The energy release in cycle is: removal heat

The ambient temperature is 289 K, 1atm and temperature of SSPCM layer is assuming a constant temperature 303 K, the optimal time (i.e. Melting/fusing temperature, and its latent capacity is 265MJ/m^3。The initial condition (t=0) of indoor air temperature is assuming 289 K。

Each time increment $\triangle$ t is 0.1 sec, then iterations up to the time we set, and need to satisfy the convergence criteria.

3.6 Boundary Conditions

Using the embedding macro files of the Fluent to select our boundary conditions and our case is unsteady. And the maximum of solar radiation on the south wall is 900Wm^{-2} and the Hsin-Chu city in summer wind speed is southern 6 ms^{-1} 、average out door temperature is 302.96 K in winter wind speed is southern 6.6 ms^{-1} 、average out door temperature is 288.9 K (see Table 2)。

3.7 Convergence criteria

For the purposes of solving any number of flow field changes in the iterative process, Simulation convergence criteria as shown in Table 3.

4 Result And Discussion

4.1 Simulated Temperature Results Of Active ABE

Fig. 12 is the comparison of temperature distribution of active ABE for the fan was on (above) and off (below) in the summer. The gap is between solar panels and the TE wall as the hot side. The temperature can reach 313 to 318 K. Another side of TE produced the cooling effect, and through air-conditioning spread cool air to indoor space. Take the temperature condition at Y = 1.2m. The indoor temperature is 302 to 305 K with fan turning on, or the indoor temperature is about 304 to 307 without turning on the fan. The

results show the fan can speed up TE cooling cold-side to spread quickly to the entire room.

4.2 Simulated PMV Results Of Active ABE

ISO 7730 has recommended the use of the comfort indicators PMV (Predicted Mean Vote):

PMV provides for an average reference, to measure the comfortableness of human body in an environment. PMV index produced from many different testers, in the specific measurement environment, their subjective assessment for a number of environmental conditions. It is divided into seven stages, ranging from -3 (very cold) extends to +3 (extremely warm), neutral point of 0 for moderate heat conditions.

Fig. 13 is the PMV value when turning on and off the fan, i.e., the smaller the value of PMV, the more satisfaction. When the fan was on the indoor PMV value was about 0.69 to 1. When the fan was off the indoor PMV value was about 0.5 to 0.9.

4.3 Simulated Temperature Results Of Passive SSPCM

The energy stored in cycle is: absorption heat

The ambient temperature is 303 K, 1atm and temperature of SSPCM layer is assuming a constant temperature 293 K, the optimal temperature (ie. melting/fusing temperature, and its latent capacity is 265MJ/m^3。The initial condition (t=0) of indoor air temperature is assuming 303 K。Fig. 14 (a~e) simulated indoor air temperature vs. time (YZ plane at middle X) for the SSPCM in an energy stored cycle. At this time, initially t = 0, indoor air temperature is bigger than temperature of SSPCM layer, then all SSPCM layers start to absorb heat, Numerical results show as time increasing and the average indoor temperature will decrease. The average indoor temperature from 303 K drops to 295.93 K within 60 minutes. It produces cooling effect in the daytime or say in the summer. Except the average indoor temperature includes temperatures of wall-concrete 、 floor-wood 、 floor-air 、 door-wood and window-glass were tabulated in Table 4.

On the contrary,

The energy release in cycle is: removal heat

The ambient temperature is 289 K, 1atm and temperature of SSPCM layer is assuming a constant temperature 303 K, the optimal time (i.e. Melting/fusing temperature, and its latent capacity is 265MJ/m^3。The initial condition (t=0) of indoor air temperature is assuming 289 K。Fig. 15 (f~j) simulated indoor air temperature vs. time (YZ plane at middle X) for the SSPCM in an energy released cycle. At this time, initially t = 0, indoor air temperature is smaller than temperature of SSPCM layer, then all SSPCM layers start to release heat, Numerical results show as time increasing and the average indoor temperature will increase. The average indoor temperature from 289 K climbs to 298.8 K within 60 minutes. It produces heating effect at night time or say in the winter. Except the average indoor temperature includes temperatures of wall-concrete 、 floor-wood 、 floor-air 、 door-wood and window-glass were tabulated in Table 5.

4.4 Comparison Between Numerical And Analytical Results For Hourly Variation Of Outdoor Air Temperature

Both of above discussions of SSPCM are idealized cases since the temperature of SSPCM was forced as constant, therefore latent heat capacity will be melting or fusing in a short period of time, and the temperature difference of the average indoor temperature will be large around 8 K to 9 K. In fact the average indoor temperature will be sinusoidal cycle with relation to optimal SSPCM temperature. The temperature differences of the average indoor temperature of both energy stored cycle and energy released cycle will around 2 K to 4 K. The analytical results have been reported by Xiao [25]. Therefore we can compare our numerical results with each other based upon hourly variation of outdoor air temperature in Hsin-Chu city on one day of July. (in here, indoor air temperature is simplified equal to outdoor air temperature). From Fig. 16 shows results of numerical and analytical are pretty consistent with each other.

5 Conclusions

The above numerical results coincide with each other. The active ABE system; a building installed the ABE system wind, solar driven, bypass the

windmill flow as a air flow, ambient temperature, is equal to 308 K and indoor air temperature, 301 K. Numerical results show the indoor air temperature will decrease 2 K when the ABE operating with heat sinks, without fan. As fan is opened, strong convective heat transfer indoor air temperature will decrease approximately 4 K to 5K. Similarly, the hybrid system integrates the passive SSPCM system. The temperature differences of the average indoor temperature of both energy stored cycle and energy released cycle will around 2 K to 4 K. Hence the hybrid system will increase the function of ventilation. In comparison to natural convection, COP increases significantly, and it is quiet、 clean、 energy-saving and cost-saving. Therefore, this study established a closer to the actual physical situation in Hybrid system as a whole, including sub-systems in this new analysis. Several brief summary as:

(1) The Hybrid system's BIPV、TE、SSPCM heat sink efficiency gains can achieve energy-efficiency and clean. It can also reduce the CO_2 emissions.
(2) The Hybrid system can reduce the total input power and achieve proactive approach to achieve energy saving goals.
(3) SSPCM consists of paraffin as dispersed PCM and high-density polyethylene (HDPE) or other materials as supporting material. The total stored energy is comparable with that of traditional PCMs.
(4) SSPCM of ceiling and floor can use the same material, temperature range between 297 K to 300 K start energy stored cycle, and temperature range between 289 K to 293 K start energy released cycle.
(5) Reduce the temperature gradient between ceiling and floor to under 4 K will increase the comfortableness
of humans.
(6) 297 K is the most comfortable temperature.

6. ACKNOWLEDGEMENT

We hereby express our thanks to the National Science Council for the support of research project NSC98-2221-E-216-047.

REFERENCES

[1] H. P. Garg, S. C. Mullick and A. K. Bhargava, Solar thermal energy storage, D. Reidel Publishing Co., 1985.
[2] Project Report. Energy conservation through thermal energy storage, *An AICTE Project*, 1997.
[3] J. Stefan Uber einge problem der theoric der warmeleitung, S. B. Wein, *Acad. Mat. Natur.* 98:173–484, 1989.
[4] H. Inaba and P. Tu Evaluation of thermophysical characteristics on shape-stabilized paraffin as a solid/liquid phase-change material. *Heat Mass Transfer*; 32(4)307-12 ,1997.
[5] H. Ye and X. S. Ge, Preparation of polyethylene–paraffin compound as a form-stable solid–liquid phase change material, *Solar Energy Mater Solar Cells*; 64(1):37–44 , 2000.
[6] Y. P. Zhang, R. Yang, H. F. Di, K. P. Lin, X. Xu and P. H. Qin., Preparation, thermal performance and application of shape-stabilized PCM in energy efficient buildings. ,Collection of technical papers—2nd *International energy conversion engineering conference AIAA,* vol. 1 p. 600–610, 2004.
[7] X. Xu, Y. P. Zhang, K. P. Lin, H. F. Di and R.Yang, Modeling and simulation on the thermal performance of shape-stabilized phase change material floor used in passive solar buildings., *Energy Build*; 37:1084–91, 2005.
[8]Central Weather Bereau, Taipei, Taiwan: http://www.cwb.gov.tw/, 2008.
[9] B. Diaconu, M. Cruceru, Phase Change Material (PCM) composite insulating panel with high thermal efficiency, in: *Proceedings of the International Conference on Energy and Environment Technologies and Equipment* EEETE-17,2010. http://www.wseas.us/e-library/conferences/2010/Bucharest/EEETE/EEETE-17.pdf
[10] H. Dehra, The Electrodynamics of a Pair of PV Modules with Connected Building Resistance, Proc. of *the 3rd IASME/WSEAS Int. Conf. on Energy, Environment, Ecosystems and Sustainable Development,* Agios Nikolaos, Greece, July 24-26, 2007. http://www.wseas.us/e-library/conferences/2007creteeeesd/papers/562-125.pdf
[11] A. A. Voevodin, C. Muratore and S. A. Aouadi, Thermal Load Adaptive Surfaces with Microencapsulated Phase Change Materials, in: *Proceedings of the 7th IASME / WSEAS International Conference on Heat Transfer, Thermal Engineering and Environment* (HTE '09), 2009. http://www.wseas.us/e-library/conferences/20

09/moscow/HTE/HTE05.pdf
[12] S. Van Dessel, A. Messac and R. Khire, Active building envelopes: a preliminary analysis, in: *Asia International Renewable Energy Conference*, Beijing, China, 2004.
[13] B. J. Tsai and J. H. Lee, Active Building Envelope System(ABE): Wind & Solar driven Ventilation 、 Electricity 、 Heat pump, *Proceeding of the 25th National Conference on Mechanical Engineering*, The Chinese Society of Mechanical Engineers, Da-Yeh Univ. 2008. (NSC 96-2221-E-216-015)
[14] G. B. Zhou, Y. P. Yang, X. Wang and S. X. Zhou, Numerical analysis of effect of shape-stabilized phase change material plates in a building combined with night ventilation, *Applied Energy,* Vol. 86, pp.52-59, 2009.
[15] G. Comini, et al., Finite element of non-linear heat conduction problems with special reference to phase change., *Int. J Number Meth Eng*; 8:613–24, 1974.
[16] Wen, J. W. Sheffled and M. P. O'Dell. Analytical and experimental investigation of melting heat transfer. , *J Thermophys*; 3:330–9, 1989.
[17] C. R. Swaminathan and V. R. Vollar, On the enthalpy method, *Int. J Num Meth Heat Fluid Flow*; 3:233–44, 1993.
[18] V. R. Vollar, et al., An enthalpy method for convection, fusion phase change, *Int J Numer Meth Eng*; 24:271–84, 1987.
[19] G. B. Zhou, Y. P. Yang, K. P. Lin and W. Xiao, Thermal analysis of a direct gain room of shape-stabilized PCM plates, *Renewable Energy,* Vol. 33, pp.1228-36, 2008.
[20] ASHRAE. ASHRAE handbook – Fundamentals, Chapter 3: Heat transfer. Atlanta: *ASHRAE*; 2001.
[21] Oppenheim AK. Radiation analysis by network method. Trans; *ASME* 195665:725–35.
[22] J. P. Holman. Heat transfer. 8th ed. New York: McGraw-Hill; 1997.
[23] C. K. Wilkins, R. Kosonen and T Laine, An analysis of office equipment load factors, *ASHRAE J.* , 33:38–44, 1991.
[24] B. Zivkovic and I.Fujii, An analysis of isothermal phase change of phase change material within rectangular and cylindrical containers, *Solar Energy,* 70:51–61, 2001.
[25] W. Xiao, X. Wang and Y. Zhang, Analytical optimization of interior PCM for energy storage in a lightweight passive solar room, *Applied Energy*, 86:2013–2018, 2009.

Figures

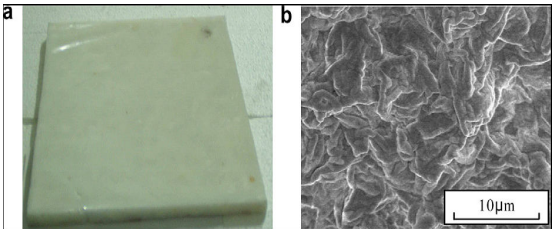

Fig. 1. The photos of the shape-stabilized PCM: (a) photo of the PCM plate; (b) electronic microscopic picture by scanning electric microscope (SEM) [6]

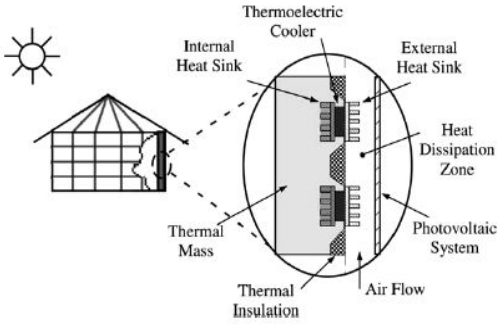

Fig. 2. Active building envelope (ABE) system [12]

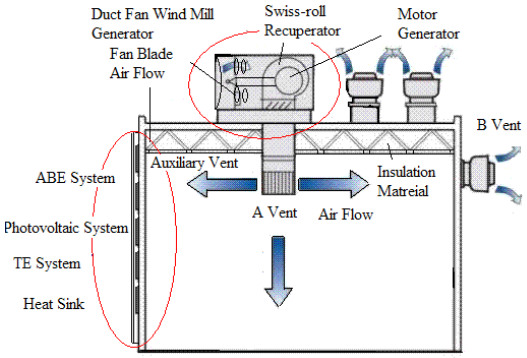

Fig. 3. Active building envelope (ABE) system with ventilation effect (Fan) [13]

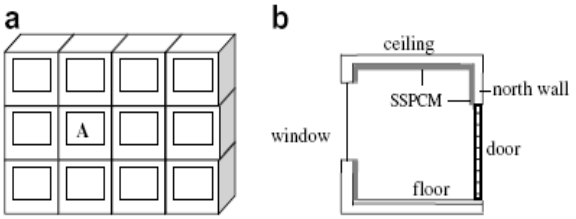

Fig. 4. Schematic of the simulated room: (a) location of the simulated room A in the building and (b) profile of the room A with SSPCM.

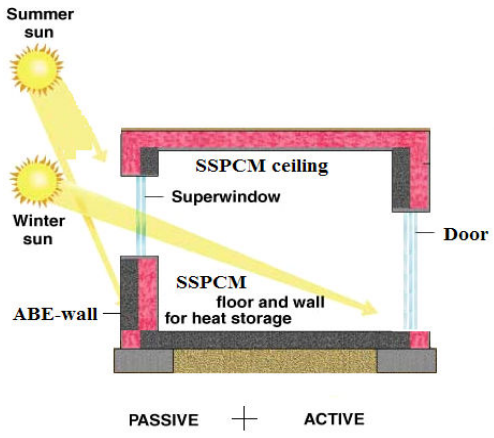

Fig. 5. Schematic of the simulated room with Hybrid system: profile of the room A with SSPCM and ABE wall

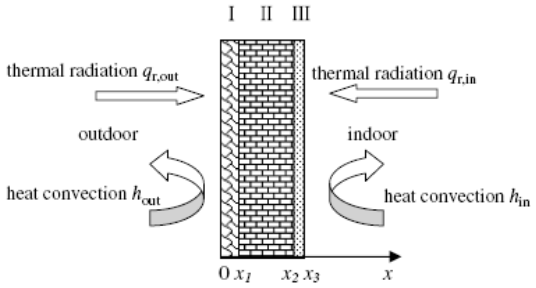

Fig. 6 Exterior wall surface

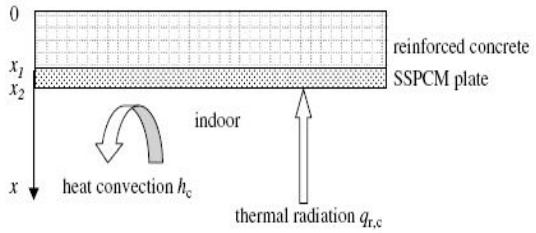

Fig. 7 Schematic of the ceiling heat transfer

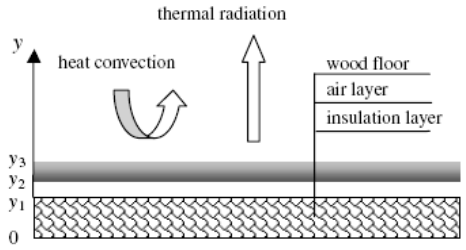

Fig.8 The floor

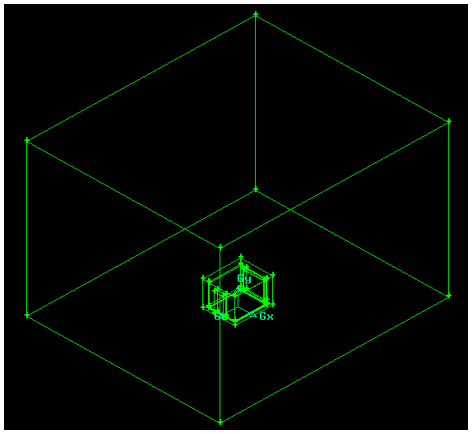

Fig. 9 : Schematic diagram of computational domain means environments surrounding the model room。

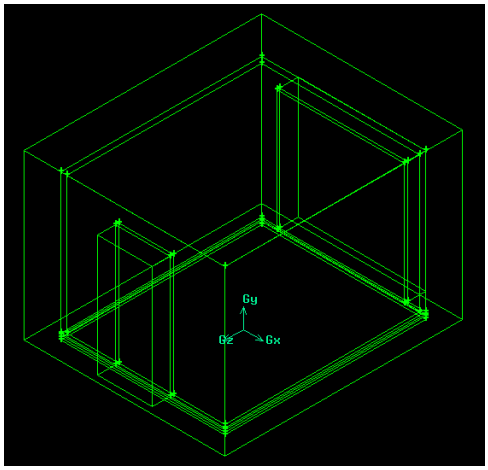

Fig.10：Schematic diagram of the model room for analysis of a building。

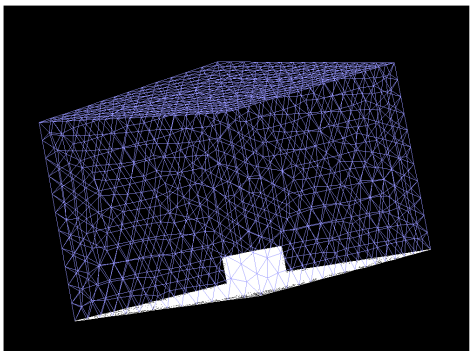

Fig.11 ： Grid mesh of the model room and environments

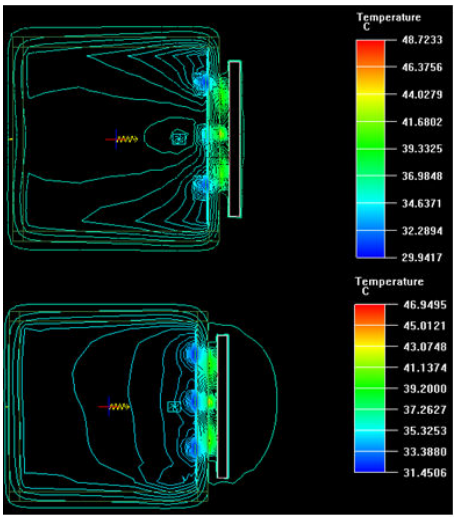

Fig. 12 Comparison of temperature distribution of the active ABE system for the fan was on (above) and off (below)

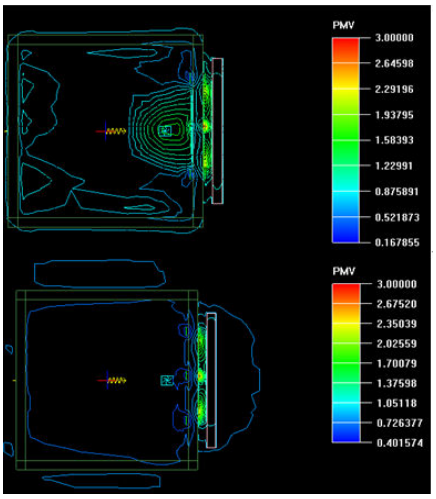

Fig. 13 the PMV value when turning on (above) and off (below) the fan

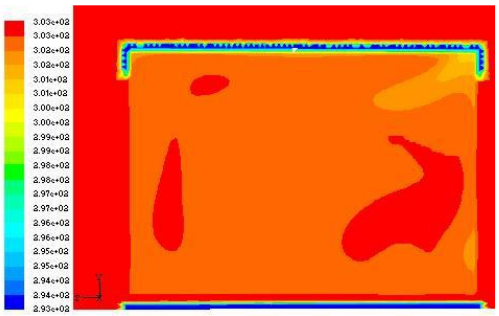

(a) 1 minute

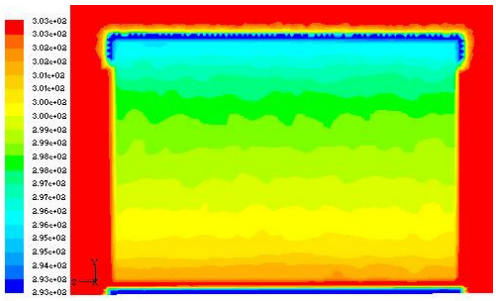

(b)10 minutes

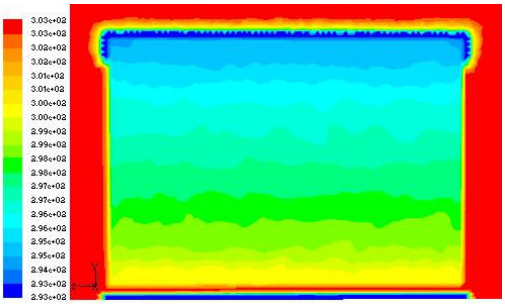

(c) 20 minutes

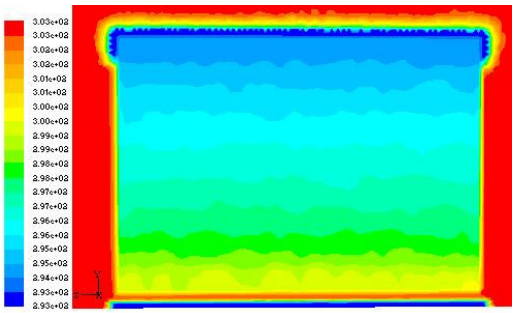

(d) 30 minutes

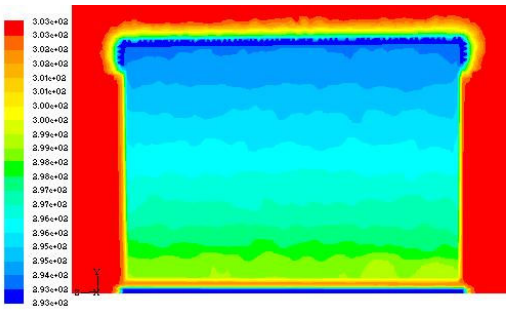

(e) 60 minutes

Fig. 14 (a~e) Simulated indoor air temperature vs. time

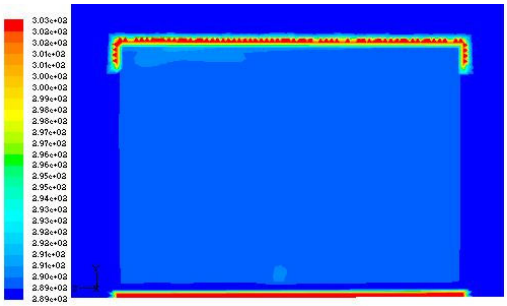

(f) 1 minute

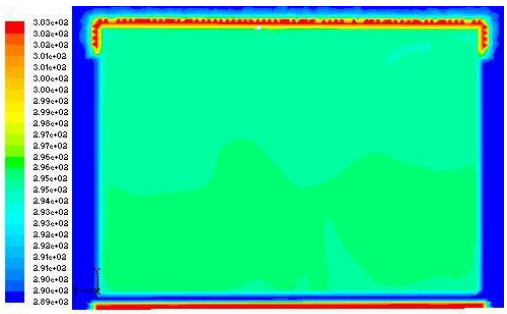

(g) 10 minutes

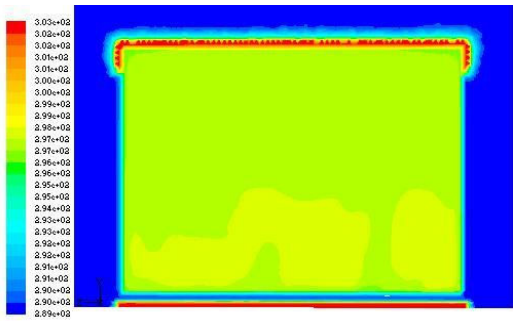

(h) 20minutes

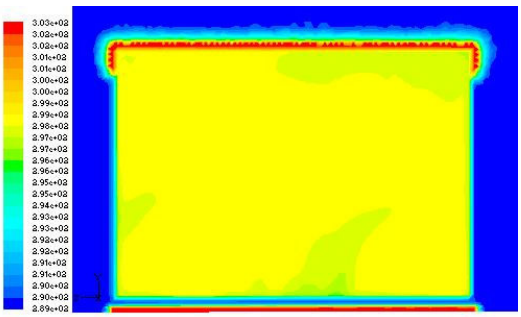

(i) 30 minutes

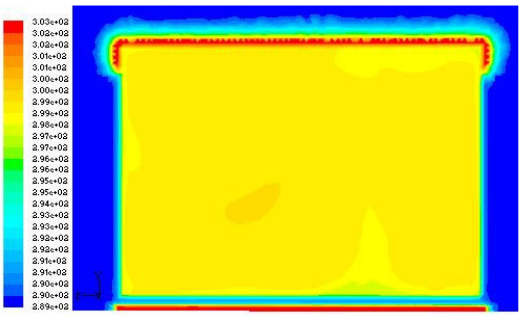

(j) 60 minutes

Fig. 15 (f~j) Simulated indoor air temperature vs. time

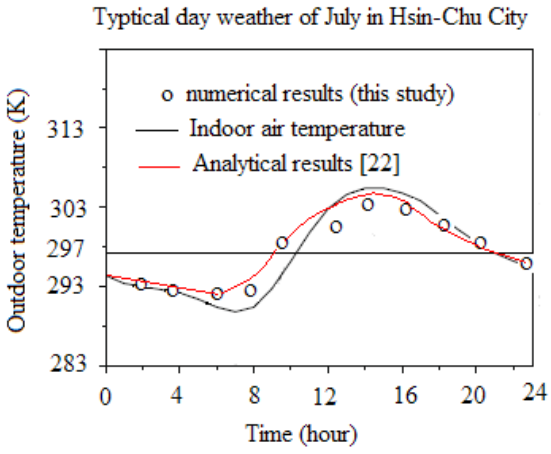

Fig. 16 hourly variation of outdoor air temperature

in Hsin-Chu City。

Table 1：Material properties of the building

Materials	P (kgm^{-3})	C_p ($kJkg^{-1}℃^{-1}$)	K ($Wm^{-1}℃^{-1}$)	U ($Wm^{-2}□^{-1}$)
SSPCM	850	1.0	0.2	-
Concrete	2500	0.92	1.75	-
Window / Glass	1400	1.05	0.58	3.01
Door /Wood	500	2.5	0.14	0.875

Table 2：Weather data of Hsin-Chu City

Season	Temperature (□)	Wind speed (ms^{-1})	Pressure (Pa)
Summer	29.6	6 (Southern wind)	1044.8
Winter	15.9	6.6 (Northern wind)	1017

Table 3： Convergence criteria

continuity	x-velocity	y-velocity	z-velocity	energy
0.001	0.001	0.001	0.001	1e-06

Table 4: Average indoor air temperature vs. time for SSPCM storage energy, absorption heat

Time min	concrete	indoor-air	floor-wood	floor-air	door-wood	Window glass
1	302.97	302.35	302.97	298.00	302.99	302.99
5	302.88	300.27	302.85	297.91	302.96	302.95
10	302.78	298.60	302.71	297.82	302.91	302.90
20	302.60	296.99	302.42	297.66	302.81	302.80
30	302.45	296.38	302.14	297.51	302.70	302.69
60	302.08	295.93	301.37	297.12	302.40	302.40

Table 5: Average indoor air temperature vs. time for SSPCM release energy, removal heat

Time min	concrete	inside-air	floor-wood	floor-air	door-wood	Window glass
1	289.03	289.83	289.03	296.00	289.00	289.01
5	289.16	292.78	289.19	296.06	289.05	289.06
10	289.30	295.09	289.40	296.17	289.12	289.13
20	289.55	297.28	289.83	296.41	289.26	289.28
30	289.76	298.12	289.27	296.63	289.40	289.43
60	290.29	298.80	291.47	297.25	289.82	289.84

Dr. Bor-Jang Tsai is currently Professor of Mechanical Engineering at Chung Hua University in HsinChu, Taiwan, Republic of China. Dr. Tsai earned his Ph.D from the School of Aerospace and Mechanical Engineering University of Missouri- Columbia in 1992, and had his M.S and B.S. in Mechanical Engineering from Clemson University, and Tatung University in 1984 and 1981, respectively. Professor Tsai's research interests cover: (1) Active building envelope system(ABE) : Wind & solar driven ventilation、electricity、heat pump (2) Study of parameters affecting thermoelectric module performance (3) Hybrid structural systems of an active building envelope system(ABE) (4) Design and aerodynamic analysis of a flapping wing micro aerial vehicle (5) A Novel swiss-roll recuperator for the micro-turbine engine (6) Performance of a half-height innovative cooling Fan. Most of his researches are in areas of thermal fluid science, renewable energy, aerodynamic, gas turbine and green buildings.